

Article

# The Modification of the Runner and Ingate Geometry to eliminate Misrun Defects on the Piston using Gravity Die Casting

Vika Rizkia <sup>1\*</sup>, Muhammad Fernanda Alvi Yasin <sup>1\*</sup>, Nabila Banowati <sup>1</sup>, Veronika Noviaty <sup>1</sup>

<sup>1</sup> Mechanical Engineering, Politeknik Negeri Jakarta, Kampus UI, Depok, 16425

\* Correspondence: [vika.rizkia@mesin.pnj.ac.id](mailto:vika.rizkia@mesin.pnj.ac.id); [muhammadfernanda5@gmail.com](mailto:muhammadfernanda5@gmail.com)

**Abstract:** Piston is an essential component of an engine because it plays a crucial role in the combustion process that drives the motorcycle. Gravity dies casting has become an ideal method for producing pistons owing to its high-quality product, cost-effective with excellent dimensional accuracy, good surface finish, and performance characteristics. However, misrun defect may occur during metal filling and solidification. This study aims to find the suitable dimensions for motorcycle piston products without the presence of misrun using MAGMASoft. The geometry modification introduced in this research are an ingate area of 176, 264, and 352 mm<sup>2</sup> as well as the angle of runner of 60, 160, and 180°. Modifying the ingate area to 264 mm<sup>2</sup> and the angle of the runner to 160° eliminated the misrun defect in the piston product. This phenomenon results from the laminar flow, higher temperature, and quicker flow velocity of the molten metal as it fills the window (the thinnest part of the piston).

**Keywords:** Casting; Piston; Runner; Ingate; Misrun Defect

**Citation:** Rizkia, V., Fernanda Alvi Yasin, M., Banowati, N., & Noviaty, V. (2023). The Modification of the Runner and Ingate Geometry to eliminate Misrun Defects on the Piston using Gravity Die Casting. *Recent in Engineering Science and Technology*, 1(02), 1–11. <https://doi.org/10.59511/riestech.v1i0.2.13>

Academic Editor: Iwan Susanto

Received: 6 February 2023

Accepted: 3 March 2023

Published: 1 April 2023

**Publisher's Note:** MBI stays neutral with regard to jurisdictional claims in published maps and institutional affiliations.



**Copyright:** © 2023 by the authors. Licensee MBI, Jakarta, Indonesia. This article is an open access article distributed under MBI license (<https://mbi-journals.com/licenses/by/4.0/>).

## 1. Introduction

The motorcycle piston is a vital component of an engine as it plays a critical role in the combustion process that powers the motorcycle. The piston is responsible for converting the energy from the burning fuel and air mixture into mechanical motion by moving up and down inside the engine's cylinder[1]. Gravity dies casting is an ideal method for producing high-quality, cost-effective pistons with excellent dimensional accuracy, surface finish, and performance characteristics[2]–[4]. However, in addition to the inherent benefits, various defects such as misrun, shrinkage, inappropriate filling, porosity, blow holes, and pin holes may occur during metal filling and solidification[5], [6]. According to reports, ninety percent of these casting flaws result from improper casting design [7]–[10], which influences mold filling and affects the mechanical properties of the cast pieces[11], [12].

Due to the importance of mold filling, numerous studies have been conducted in this field. Mold filling is affected by fluid flow pattern, gating design, and solidification[13], [14]. Masoumi et al. [15] reported that alterations in gating system configuration result in a divergence of melt flow from the mold's parting line, altering the mold filling pattern. According to Rajput et al. [16], gate geometry influences the change of metal head pressure at the mold cavity entrance. The design of the gate influences metal filling, which directly affects casting quality. The correct gating design produces a uniform heat gradient and prevents mold erosion, producing smooth metal flow. Precise gate sizes and designs minimize air entrapment by controlling the entry velocity of molten metal.

In addition, numerous researchers have developed mathematical models to

overcome the casting defects mentioned above [17]–[21]. These mathematical models have been implemented as software. MAGMASoft is one such program renowned for its virtual casting simulation and optimization capabilities[22]. With such tools, numerical simulations were conducted to identify flaws virtually. These virtual simulations aid in the reduction of casting flaws, which benefits manufacturers in numerous ways. Vijayaram et al. [23] examined computer simulations' use to detect casting defects that develop during the solidification phase of casting components. They demonstrated that such simulations greatly benefited the foundry industry. Gunasegaram et al. [24] determined the essential elements that influence the shrinkage porosity in permanent mold castings utilizing numerical simulation and experimental design to achieve an optimum result. They discovered that a thick mold layer combined with a high mold temperature significantly shifted the shrinkage porosity away from important locations. Dabade et al. [25] employed the design of experiments and the Taguchi technique to identify the main process parameter influencing the casting process. In order to lessen the degree of shrinkage porosity in the cast component, they performed a solidification study with novel gating and feeding systems using computer simulation software. Their results demonstrated a significant decrease in shrinkage porosity and an improvement in casting yield.

Among other similar studies, in this research, the numerical simulation technique was applied to the gravity die casting of a cast component to diminish the misrun defect. The component considered for the investigation was a motorcycle piston. The cast component was realistically simulated using MAGMASoft, and the simulation results were implemented in real-time casting.

## 2. Materials and Experiment Methods

The present investigation is performed to find the proper dimensions of the runner and ingate in the motorcycle piston case, which is being processed in the gravity die casting route, and resolve the misrun defects identified using MAGMASoft. The three-dimensional CAD model and the actual product of the initial piston casting are shown in Figure. 1. In addition, the material specifications and gating system parameters are seen in Table.1.

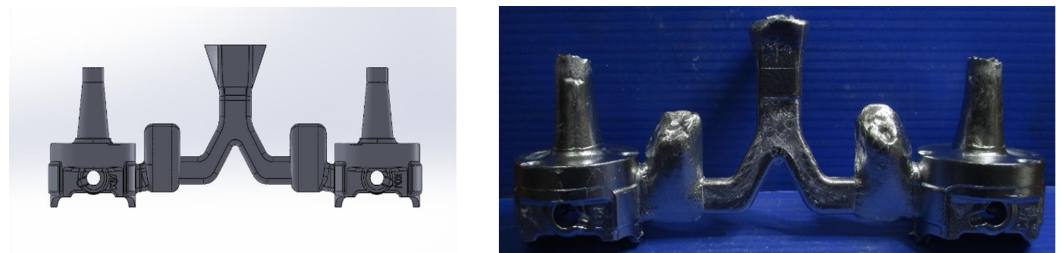


**Figure 1.** (a) 3D models of the piston and the gating system, (b) as cast piston

**Table 1.** Material specifications and gating system parameter

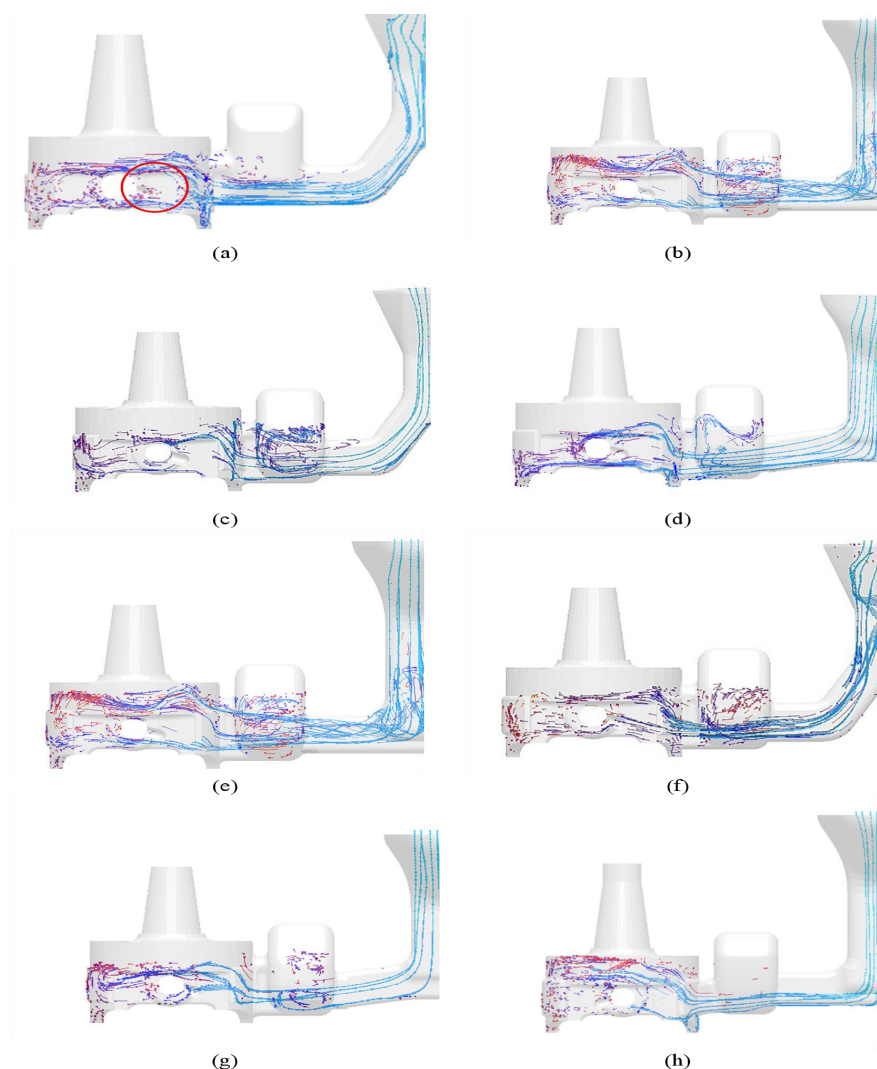
Cast Material	A351
Dies Material	H13
Pouring Temperature	760°C
Dies Core Temperature	350°C
Piston weight (1 cavity)	0.6 kg

Piston height	76 mm
Sprue height	67 mm
Ingate area	164 mm <sup>2</sup>
Angle of runner	60°

In this study, the initial design was modified in order to diminish misrun defect within the cast product by changing the ingate area of 176, 264, and 352 mm<sup>2</sup> as well as the angle of runner of 60, 160, and 180°.

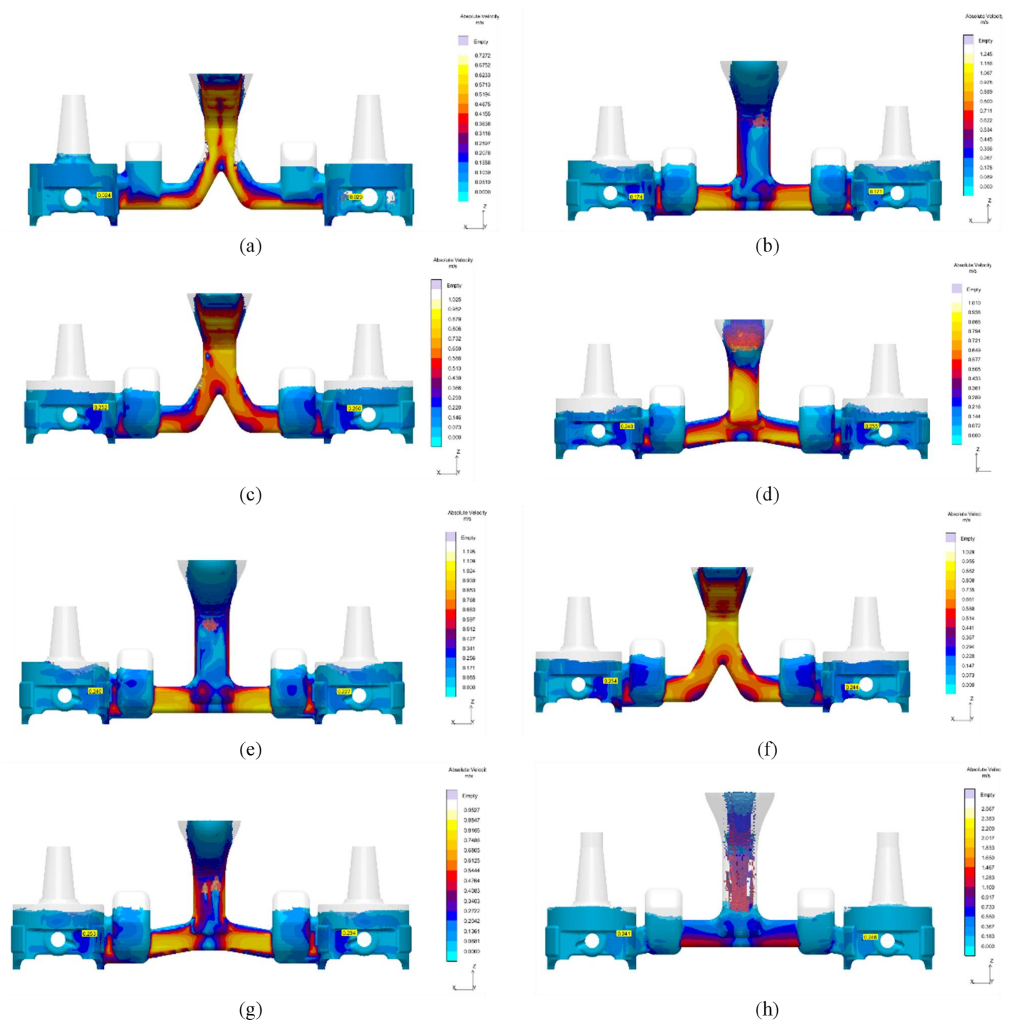
### 3. Results and Discussion

#### 3.1. Flow Tracer



**Figure 2.** The flow tracer of (a) original design, (b) ingate area of 352 mm<sup>2</sup> and angle of the runner of 180°, (c) ingate area of 352 mm<sup>2</sup> and angle of the runner of 60°, (d) ingate area of 352 mm<sup>2</sup> and angle of the runner of 160°, (e) ingate area of 176 mm<sup>2</sup> and angle of the runner of 180°, (f) ingate area of 176 mm<sup>2</sup> and angle of the runner of 60°, (g) ingate area of 176 mm<sup>2</sup> and angle of the runner of 160°, (h) ingate area of 264 mm<sup>2</sup> and angle of the runner of 180°, (i) ingate area of 264 mm<sup>2</sup> and angle of the runner of 60°, (j) ingate area of 264 mm<sup>2</sup> and angle of the runner of 160°

In the 1st – 8th modification designs depicted in Figure 2 (b)-(i), turbulence flow is still present. However, in the 9th modification, which involves changes in the geometry of the ingate area of 264 mm<sup>2</sup> and a runner angle of 160° as seen in Figure 2 (j), there is no visible turbulence flow. In addition, in the flow tracer analysis of the 9th modification, the flow of material filling the product is uniform and stable, particularly in the narrow profile area (the window) where defects such as misrun are critical.



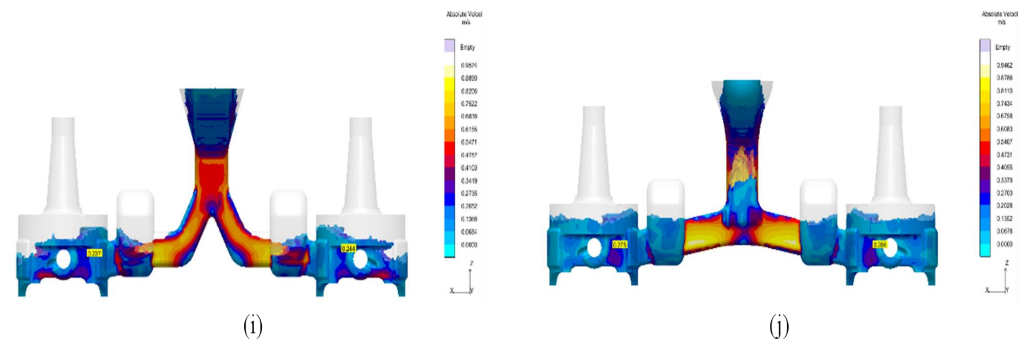


**Figure 3.** The flow velocity of (a) original design, (b) ingate area of 352 mm<sup>2</sup> and angle of the runner of 180°, (c) ingate area of 352 mm<sup>2</sup> and angle of the runner of 60°, (d) ingate area of 352 mm<sup>2</sup> and angle of the runner of 160°, (e) ingate area of 176 mm<sup>2</sup> and angle of the runner of 180°, (f) ingate area of 176 mm<sup>2</sup> and angle of the runner of 60°, (g) ingate area of 176 mm<sup>2</sup> and angle of the runner of 160°, (h) ingate area of 264 mm<sup>2</sup> and angle of the runner of 180°, (i) ingate area of 264 mm<sup>2</sup> and angle of the runner of 60°, (j) ingate area of 264 mm<sup>2</sup> and angle of the runner of 160°

The flow velocity in the MAGMASOFT program depicts the material flow rate during mold filling and the spread of the molten flow toward the product. If the flow velocity is low when filling the mold, as in the case of thin profiles or window sections of the product, premature solidification may occur. Figure 3 depicts the flow velocity in both the initial design as well as modified designs. Figure 3(a) demonstrates that molten metal enters the gating system (ingate) unevenly at 1.244 seconds. In addition, a very low flow velocity occurs in the thin profile of the product, which is 0.024 m/s, causing incomplete casting or misrun.

Figure 3 (b)-(j) and Table 2 show the flow velocity results in the window for various design modifications. The slower the flow velocity of the molten metal in filling the window, the higher of misrun occurrence. Therefore, based on the simulation results, the best flow velocity is in 9th modification, which has an ingate area of 264 mm<sup>2</sup> and a runner angle of 160° with a value of 0.275 m/s.

**Table 2.** Molten flow velocity on windows in modification designs

Modification	Ingate Area (mm <sup>2</sup> )	Angle of Runner (°)	Flow Velocity (m/s)
1	352	180	0.174
2	352	60	0.237
3	352	160	0.255
4	176	180	0.24
5	176	60	0.244
6	176	160	0.253
7	264	180	0.241
8	264	60	0.244
9	264	160	0.275



### 3.3. Pouring Temperature

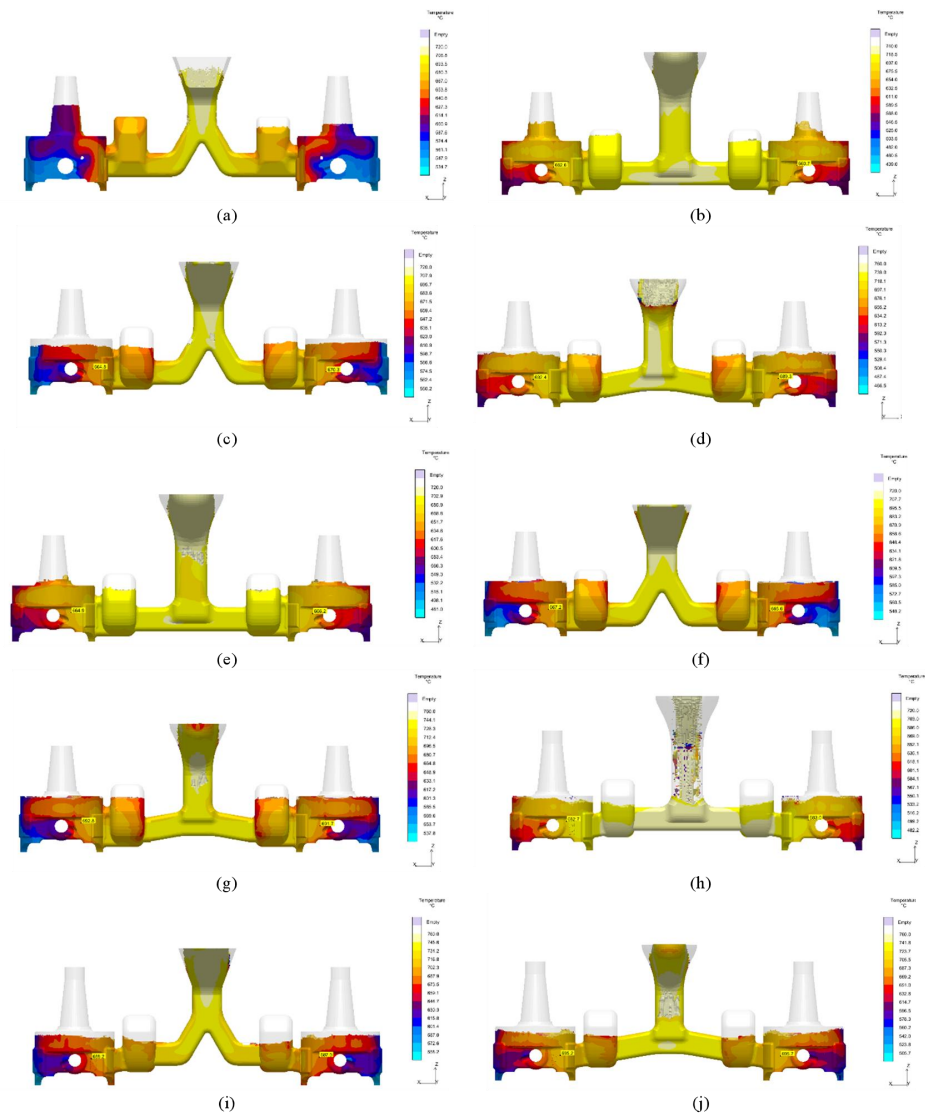


**Figure 4.** The pouring temperature of (a) original design, (b) ingate area of 352 mm<sup>2</sup> and angle of the runner of 180°, (c) ingate area of 352 mm<sup>2</sup> and angle of the runner of 60°, (d) ingate area of 352 mm<sup>2</sup> and angle of the runner of 160°, (e) ingate area of 176 mm<sup>2</sup> and angle of the runner of 180°, (f) ingate area of 176 mm<sup>2</sup> and angle of the runner of 60°, (g) ingate area of 176 mm<sup>2</sup> and angle of the runner of 160°, (h) ingate area of 264 mm<sup>2</sup> and angle of the runner of 180°, (i) ingate area of 264 mm<sup>2</sup> and angle of the runner of 60°, (j) ingate area of 264 mm<sup>2</sup> and angle of the runner of 160°

$$a = 1, \quad (1)$$

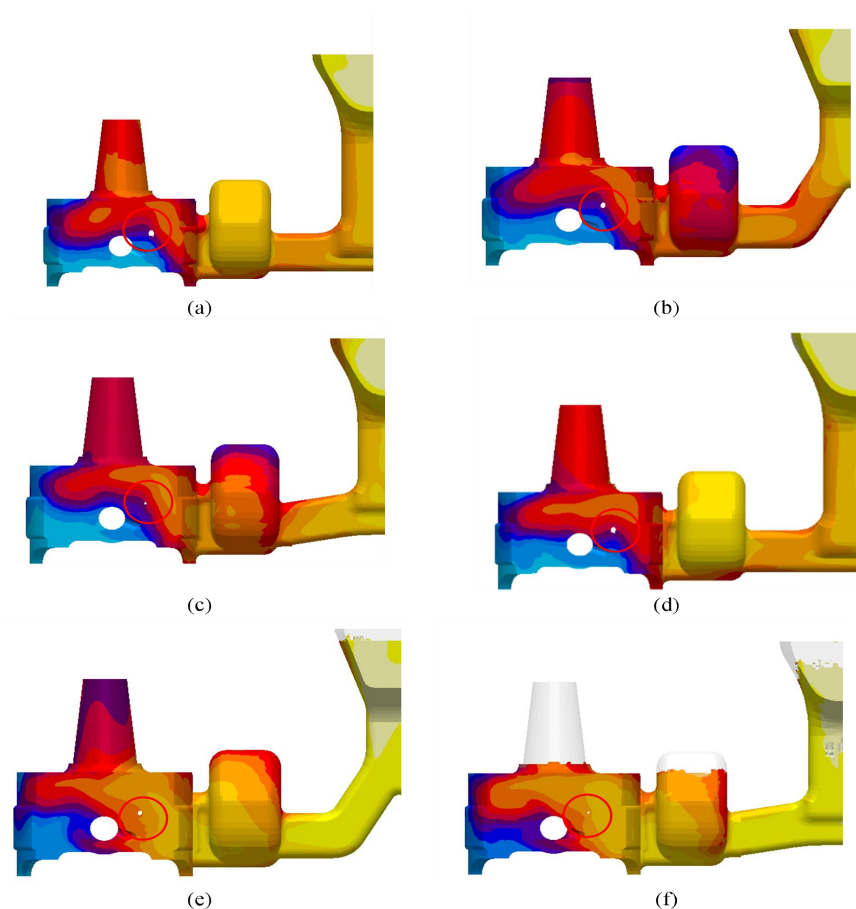
The pouring temperature on MAGMASOFT shows temperature changes when molten metal enters the mold during the casting process. The temperature changes in the thin profile, window, significantly affect the casting product. If the window profile (thin part) shows a lower temperature than the others, it will result in premature solidification, leading to a misrun defect. Figure 4(a) shows that the initial solidification occurred on the thin profile of the product, far from the ingate, which appears blue. When the molten metal had filled the product, non-uniform temperature changes occurred in the thinnest part of the product. In addition, that part indicates premature solidification due to low temperature. It resulted in incomplete casting inside the piston product.

Figure 4 (b)-(j) and Table 3 show the results of temperature changes in the window for various design modifications. Low pouring temperature when filling the window mold may indicate premature solidification, leading to a misrun. Therefore, based on the simulation results, the best pouring temperature shows in the 9th modification, which has an ingate area of 264 mm<sup>2</sup> and a runner angle of 160° with a value of 695.7°C. The text continues here.

**Table 3.** Molten flow velocity on windows in various modification designs

Modification	Ingate Area (mm <sup>2</sup> )	Angle of Runner (°)	Temperature (°C)
1	352	180	662.6
2	352	60	664.8
3	352	160	689.4
4	176	180	665.9
5	176	60	667.2
6	176	160	692.8
7	264	180	664.5
8	264	60	688.2
9	264	160	695.7

### 3.3. Misrun Defect



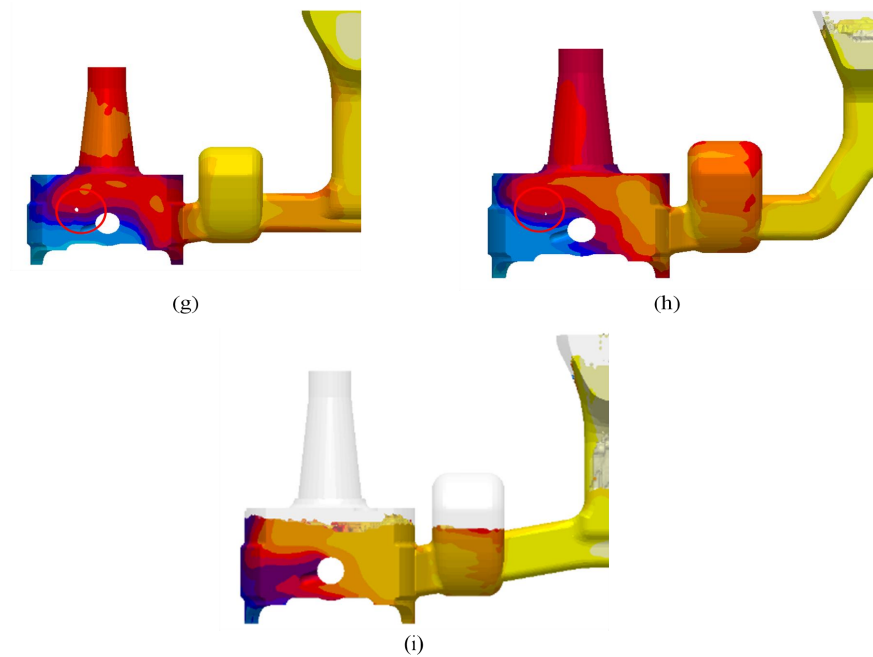


**Figure 5.** Misrun defect on all the modified designs (a) ingate area of 352 mm<sup>2</sup> and angle of the runner of 180°, (b) ingate area of 352 mm<sup>2</sup> and angle of the runner of 60°, (c) ingate area of 352 mm<sup>2</sup> and angle of the runner of 160°, (d) ingate area of 176 mm<sup>2</sup> and angle of the runner of 180°, (e) ingate area of 176 mm<sup>2</sup> and angle of the runner of 60°, (f) ingate area of 176 mm<sup>2</sup> and angle of the runner of 160°, (g) ingate area of 264 mm<sup>2</sup> and angle of the runner of 180°, (h) ingate area of 264 mm<sup>2</sup> and angle of the runner of 60°, (i) ingate area of 264 mm<sup>2</sup> and angle of the runner of 160°

Figure 5 shows the results of incomplete filling in the window area for various design modifications. As can be seen, there is a misrun presence in the 1st-8th modification due to slow flow velocity as well as low temperature in the window section of the piston. The diameters of the misrun that occurred within the piston are tabulated in Table 4. Therefore, based on the simulation results, the best geometry modification is shown in the 9th modification, which has an ingate area of 264 mm<sup>2</sup> and a runner angle of 160° with no misrun appearing. This phenomenon is due to the geometry modification providing a uniform filling as well as avoiding incomplete casting inside the thin section of the piston.

**Table 4.** The diameters of misrun that occurred within the piston window

Modification	Ingate Area (mm <sup>2</sup> )	Angle of Runner (°)	Diameter of misrun (mm <sup>2</sup> )
1	352	180	6.3
2	352	60	3.92
3	352	160	0.84
4	176	180	4.96
5	176	60	2.52
6	176	160	0.56
7	264	180	2.55
8	264	60	0.63
9	264	160	0



### 3.4. Piston casting

**Table 5.** Comparison between the initial design product and the modified product with ingate area of 264 mm<sup>2</sup> and angle of the runner of 160°



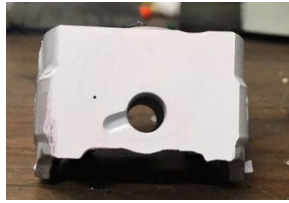
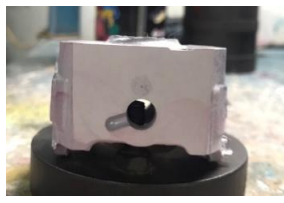






Part	Initial Piston (ingate area of 164 mm <sup>2</sup> and angle of the runner of 60°)	Modified Piston (ingate area of 264 mm <sup>2</sup> and angle of the runner of 160°)
Crown	 A photograph of the initial piston crown, which is a circular, flat surface. To the right is a cross-sectional diagram showing a 60-degree runner angle and a red arrow indicating the flow direction.	 A photograph of the modified piston crown, which is a circular, flat surface. To the right is a cross-sectional diagram showing a 160-degree runner angle and a red arrow indicating the flow direction.
Center of pin boss (1)	 A photograph of the initial pin boss (1), showing a small circular hole. To the right is a cross-sectional diagram showing a 60-degree runner angle and a red arrow indicating the flow direction.	 A photograph of the modified pin boss (1), showing a small circular hole. To the right is a cross-sectional diagram showing a 160-degree runner angle and a red arrow indicating the flow direction.
Center of pin boss (2)	 A photograph of the initial pin boss (2), showing a small circular hole. To the right is a cross-sectional diagram showing a 60-degree runner angle and a red arrow indicating the flow direction.	 A photograph of the modified pin boss (2), showing a small circular hole. To the right is a cross-sectional diagram showing a 160-degree runner angle and a red arrow indicating the flow direction.
Pin center	 A photograph of the initial pin center, showing a small circular hole. To the right is a cross-sectional diagram showing a 60-degree runner angle and a red arrow indicating the flow direction.	 A photograph of the modified pin center, showing a small circular hole. To the right is a cross-sectional diagram showing a 160-degree runner angle and a red arrow indicating the flow direction.
As Cast	 A photograph of the initial piston as cast, showing a small circular hole. A red circle highlights a defect on the side of the piston.	 A photograph of the modified piston as cast, showing a small circular hole. A red circle highlights a defect on the side of the piston.

Table 5 compares the initial design (an ingate area of 164 mm<sup>2</sup> and the angle of the runner of 60°) and the modified design with an ingate area of 264 mm<sup>2</sup> and the runner's angle of 160°. As predicted by the simulation process, the initial design casting product has a misrun defect in the center of the left pin boss, as shown in Table 5. It occurs because the geometry of the runner and gate on the initial design produces the presence of turbulence and non-uniform flow, low temperature, as well as slow flow velocity of the molten metal while filling the window (the thinnest part of the piston), which leads to the occurrence of misrun. However, the modified design with an ingate area of 264 mm<sup>2</sup> and the angle of the runner of 160° provides laminar flow, high temperature, as well as fast flow velocity of the molten metal while filling the window.

#### 4. Conclusions

1. The misrun defect that occurred in the A351 piston product from initial design, which had an ingate area of 164 mm<sup>2</sup> and a runner angle of 60°, was successfully eliminated through a simulation process of modifying the geometry using MAGMASOFT software. The modified design has also been validated through a gravity die casting process, producing piston product without misrun.
2. Among all of the modified designs examined in this study, the modification in an ingate area of 264 mm<sup>2</sup> and the runner's angle of 160° resulted in the absence of misrun defect within the piston product. This phenomenon is due to the laminar flow, higher temperature, as well as faster flow velocity of the molten metal while filling the window (the thinnest part of the piston).

#### References

1. A. Roychoudhury, A. Banerjee, F. Khoshnaw, and P. Mishra, "An FEA material strength modelling of a coated engine piston," *Mater Today Proc*, Jan. 2021, doi: 10.1016/j.matpr.2020.11.387.
2. T. Raviteja, B. Surekha, and N. Sharma, "Influence of Cu and Al interfacing foil on Al7075/A360 FGMs fabricated by gravity casting," *Mater Today Proc*, vol. 74, pp. 1052–1056, 2023, doi: <https://doi.org/10.1016/j.matpr.2022.12.021>.
3. S. Lombardo, I. Peter, and M. Rosso, "Gravity Casting Of Variable Composition Al Alloys: Innovation And New Potentialities," *Mater Today Proc*, vol. 10, pp. 271–276, 2019, doi: <https://doi.org/10.1016/j.matpr.2018.10.406>.
4. T. Sathish and S. Karthick, "Gravity Die Casting based analysis of aluminum alloy with AC4B Nano-composite," *Mater Today Proc*, vol. 33, pp. 2555–2558, 2020, doi: <https://doi.org/10.1016/j.matpr.2019.12.084>.
5. A. S. Marodkar, H. Patil, J. Chavhan, and H. Borkar, "Effect of gravity die casting, squeeze casting and extrusion on microstructure, mechanical properties and corrosion behaviour of AZ91 magnesium alloy," *Mater Today Proc*, 2023, doi: <https://doi.org/10.1016/j.matpr.2023.03.053>.
6. A. Reis, Z. Xu, R. V Tol, and R. Neto, "Modelling feeding flow related shrinkage defects in aluminum castings," *J Manuf Process*, vol. 14, no. 1, pp. 1–7, 2012, doi: <https://doi.org/10.1016/j.jmapro.2011.05.003>.
7. S. L. Nimbulkar and R. S. Dalu, "Design optimization of gating and feeding system through simulation technique for sand casting of wear plate," *Perspect Sci (Neth)*, vol. 8, pp. 39–42, 2016, doi: <https://doi.org/10.1016/j.pisc.2016.03.001>.
8. H. Iqbal, A. K. Sheikh, A. Al-Yousef, and M. Younas, "Mold Design Optimization for Sand Casting of Complex Geometries Using Advance Simulation Tools," *Materials and Manufacturing Processes*, vol. 27, no. 7, pp. 775–785, Jul. 2012, doi: 10.1080/10426914.2011.648250.
9. H. Bhatt, R. Barot, K. Bhatt, H. Beravala, and J. Shah, "Design Optimization of Feeding System and Solidification Simulation for Cast Iron," *Procedia Technology*, vol. 14, pp. 357–364, 2014, doi: <https://doi.org/10.1016/j.protcy.2014.08.046>.

10. T. Wang, S. Yao, Q. Tong, and L. Sui, "Improved filling condition to reduce casting inclusions using the submerged gate method," *J Manuf Process*, vol. 27, pp. 108–113, 2017, doi: <https://doi.org/10.1016/j.jmapro.2017.01.013>.
11. D. G. Eskin, Suyitno, and L. Katgerman, "Mechanical properties in the semi-solid state and hot tearing of aluminium alloys," *Prog Mater Sci*, vol. 49, no. 5, pp. 629–711, 2004, doi: [https://doi.org/10.1016/S0079-6425\(03\)00037-9](https://doi.org/10.1016/S0079-6425(03)00037-9).
12. D. M. Stefanescu, "Computer simulation of shrinkage related defects in metal castings – a review," *International Journal of Cast Metals Research*, vol. 18, no. 3, pp. 129–143, Mar. 2005, doi: [10.1179/136404605225023018](https://doi.org/10.1179/136404605225023018).
13. H. Kang et al., "Effects of gate system design on pore defects and mechanical properties of pore-free die-cast Al-Si-Cu alloy," *Mater Today Commun*, vol. 31, p. 103673, 2022, doi: <https://doi.org/10.1016/j.mtcomm.2022.103673>.
14. K. S. Keerthiprasad, M. S. Murali, P. G. Mukunda, and S. Majumdar, "Numerical Simulation and Cold Modeling experiments on Centrifugal Casting," *Metallurgical and Materials Transactions B*, vol. 42, no. 1, pp. 144–155, 2011, doi: [10.1007/s11663-010-9402-4](https://doi.org/10.1007/s11663-010-9402-4).
15. M. Masoumi, H. J. Hu, J. Hedjazi, and M. A. Boutorabi, "Effect of Gating Design on Mold Filling," 2005.
16. Rajput R.K, *A Textbook of Manufacturing Technology: Manufacturing Processes*. Boston: Laxmi Publication, 2007.
17. K. Min, K. Kim, S. K. Kim, and D.-J. Lee, "Effects of oxide layers on surface defects during hot rolling processes," *Metals and Materials International*, vol. 18, no. 2, pp. 341–348, 2012, doi: [10.1007/s12540-012-2020-8](https://doi.org/10.1007/s12540-012-2020-8).
18. G. Timelli, G. Camicia, S. Ferraro, and R. Molina, "Effects of grain refinement on the microstructure, mechanical properties and reliability of AlSi7Cu3Mg gravity die cast cylinder heads," *Metals and Materials International*, vol. 20, no. 4, pp. 677–686, 2014, doi: [10.1007/s12540-014-4013-2](https://doi.org/10.1007/s12540-014-4013-2).
19. H. Yang, S. Ji, D. Watson, and Z. Fan, "Repeatability of tensile properties in high pressure die-castings of an Al-Mg-Si-Mn alloy," *Metals and Materials International*, vol. 21, no. 5, pp. 936–943, 2015, doi: [10.1007/s12540-015-5108-0](https://doi.org/10.1007/s12540-015-5108-0).
20. R. Haghayeghi, E. Ezzatneshan, H. Bahai, and L. Nastac, "Numerical and experimental investigation of the grain refinement of liquid metals through cavitation processing," *Metals and Materials International*, vol. 19, no. 5, pp. 959–967, 2013, doi: [10.1007/s12540-013-5008-0](https://doi.org/10.1007/s12540-013-5008-0).
21. M. Vlach et al., "Annealing Effects in Cast Commercial Aluminium Al-Mg-Zn-Cu(-Sc-Zr) Alloys," *Metals and Materials International*, vol. 27, no. 5, pp. 995–1004, 2021, doi: [10.1007/s12540-019-00499-6](https://doi.org/10.1007/s12540-019-00499-6).
22. J. Ha, P. Cleary, V. Alguine, and T. T. Nguyen, "Simulation of die filling in gravity die casting using SPH and MAGMASoft," *CRC for Alloy and Solidification Technology*, Jan. 1999.
23. T. R. Vijayaram, S. Sulaiman, A. M. S. Hamouda, and M. H. M. Ahmad, "Numerical simulation of casting solidification in permanent metallic molds," *J Mater Process Technol*, vol. 178, no. 1, pp. 29–33, 2006, doi: <https://doi.org/10.1016/j.jmatprotec.2005.09.025>.
24. D. R. Gunasegaram, D. J. Farnsworth, and T. T. Nguyen, "Identification of critical factors affecting shrinkage porosity in permanent mold casting using numerical simulations based on design of experiments," *J Mater Process Technol*, vol. 209, no. 3, pp. 1209–1219, 2009, doi: <https://doi.org/10.1016/j.jmatprotec.2008.03.044>.
25. U. A. Dabade and R. C. Bhedasgaonkar, "Casting Defect Analysis using Design of Experiments (DoE) and Computer Aided Casting Simulation Technique," *Procedia CIRP*, vol. 7, pp. 616–621, 2013, doi: <https://doi.org/10.1016/j.procir.2013.06.042>. Author 1, A.B.; Author 2, C.D. Title of the article. *Abbreviated Journal Name* Year, Volume, page range.